

# Chemical Relaxation and Double Layer Model Analysis of Boron Adsorption on Alumina

C. V. Toner IV and D. L. Sparks\*

## ABSTRACT

Boron is a plant nutrient essential for adequate plant growth, yet the range between B deficiency and toxicity levels is rather narrow. Boron adsorption reactions with soil components, particularly sesquioxides, most often regulate the amount of B in the soil solution. The reaction mechanisms of B adsorption on oxides have not been fully characterized, however. Pressure-jump relaxation experiments were conducted to measure the rates and determine the reaction mechanism for B adsorption on an alumina ( $\gamma\text{-Al}_2\text{O}_3$ ) surface from  $\text{B}(\text{OH})_3\text{-B}(\text{OH})_4^-$  solutions. Relaxation times ( $\tau$ ) were measured from pH 7.0 to 9.7 in alumina suspensions with  $0.012 \text{ mol L}^{-1}$  total B. A plot of  $\tau^{-1}$  vs.  $\text{B}(\text{OH})_4^-$  plus surface site concentration obtained from the triple layer model (TLM) assuming inner sphere  $\text{B}(\text{OH})_4^-$  adsorption yielded an adsorption rate constant ( $k_i^{\text{int}}$ ) of  $3.3 \times 10^5 \text{ L mol}^{-1} \text{ s}^{-1}$  and a desorption rate constant ( $k_r^{\text{int}}$ ) of  $1.8 \times 10^{-3} \text{ L mol}^{-1} \text{ s}^{-1}$ . The ratio  $k_i^{\text{int}}/k_r^{\text{int}}$  yielded an equilibrium constant ( $\log K_{\text{eq}}^{\text{int}}$ ) of 8.26, in agreement with the intrinsic equilibrium constant for  $\text{B}(\text{OH})_4^-$  adsorption ( $\log K_{\text{eq}}^{\text{int}} = 7.69$ ) obtained from adsorption isotherms. Four additional surface complexation models were tested for their ability to model both the equilibrium and kinetic data simultaneously: the constant capacitance model, the diffuse layer model, a Stern model variant, and the TLM assuming outer sphere  $\text{B}(\text{OH})_4^-$  adsorption. Only the TLM, assuming both  $\text{B}(\text{OH})_3$  and  $\text{B}(\text{OH})_4^-$  were adsorbed via ligand exchange on neutral surface sites, was successful. The TLM indicated that  $\text{B}(\text{OH})_4^-$  is the predominant adsorbed species throughout the pH range 7.0 to 10.8.

THE EQUILIBRIUM between B in the soil solution and adsorbed B plays a pivotal role in determining the amount of B available for plant uptake. Perhaps the most important soil components affecting B adsorption are soil oxides and oxyhydroxides (Keren and Bingham, 1985). The frequent occurrence of these oxides as coatings on mineral surfaces results in a physicochemical influence far in excess of what their contribution to the total soil mass would suggest, due to their highly reactive nature and great surface exposure (Sims and Bingham, 1968b). Various researchers have demonstrated the propensity of soil oxides to adsorb substantial amounts of B from solution (Goldberg and Glaubig, 1985; Rhoades et al., 1970). In a comparison of Al oxides with Fe oxides, Sims and Bingham (1968a) found that Al oxides removed nearly an order of magnitude more B from solution than Fe oxides on a weight basis. Goldberg and Glaubig (1985) studied B adsorption on several Al and Fe oxides and found that B adsorption was comparable when compared on a surface-area basis.

Although B fixation by adsorption is most often considered the dominant phenomenon in controlling B availabil-

ity, the reaction mechanisms of B adsorption have never been clearly established. Adsorption of B is believed to be specific in nature, occurring by ligand exchange with surface hydroxyl groups of variable-charge oxides and broken edges of clays (Hingston et al., 1972; Sims and Bingham, 1968a). Specific adsorption of B may occur irrespective of the sign of the net surface charge (Hingston et al., 1972).

Various models have been employed in describing B adsorption behavior in soils. These include the Langmuir equation (Bingham et al., 1971; Goldberg and Forster, 1991; Goldberg and Glaubig, 1986), as well as a phenomenological equation that assumes that two B solution species are competing for the same surface sites, boric acid [ $\text{B}(\text{OH})_3$ ] and borate [ $\text{B}(\text{OH})_4^-$ ] (Keren et al., 1981; Mezumen and Keren, 1981).

Goldberg and Glaubig (1985) have used the CCM to describe B adsorption on several Fe and Al oxides across a wide pH range (4–11). The CCM was also able to simulate B adsorption on 15 arid-zone soils (pH 5.5–11.5) using a set of surface complexation constants averaged across all 15 soils (Goldberg and Glaubig, 1986). In each application of the model to B adsorption, the researchers assumed that  $\text{B}(\text{OH})_3$  is the only B solution species adsorbed and only neutral OH sites participate in the ligand exchange, with water as the leaving ligand. Since this proposed reaction mechanism involves no charged species, surface charge has no effect on the adsorption process. Because the CCM does not consider adsorption of the background electrolyte, the B adsorption constant is only valid for a given ionic strength (Hayes et al., 1991).

Boron adsorption on kaolinite has been modeled using the TLM (Singh and Mattigod, 1992). Adsorption on kaolinite was well described by the TLM from pH 6.0 to 10.5 at constant ionic strength with either  $\text{Ca}(\text{ClO}_4)_2$  or  $\text{KClO}_4$  as the background electrolyte. Singh and Mattigod (1992) assumed that B adsorbs as both  $\text{B}(\text{OH})_3$  and  $\text{B}(\text{OH})_4^-$  in the presence of  $\text{K}^+$  and  $\text{Ca}^{2+}$ , with  $\text{B}(\text{OH})_4^-$  forming both mono- and bidentate inner sphere surface complexes. Boron adsorption on kaolinite in the presence of  $\text{Ca}^{2+}$  is enhanced by the adsorption of  $\text{Ca}^{2+}\text{-B}(\text{OH})_4^-$  ion pairs. The FITEQL program (Westall, 1982) was used to simultaneously optimize multiple equilibrium constants for B adsorption in both systems.

The TLM has been adapted by Hayes and Leckie (1987) from its original form to consider the formation of inner and outer sphere coordination complexes with the surface, a more realistic assumption considering that the specifically adsorbed ion is also a component of the EDL. In contrast

Department of Plant and Soil Sciences, Univ. of Delaware, Newark, DE 19717-1303. The authors appreciate the partial support of this research from the U.S. Borax Corporation. The senior author also acknowledges the receipt of a graduate research fellowship from the Univ. of Delaware. Received 20 Sept. 1993. \*Corresponding author (dlsparks@brahms.udel.edu).

to the inner sphere complex, which results from adsorption at the surface by ligand exchange, an outer sphere complex is an ion-pair complex between the surface and the adsorbate, with the adsorbate retaining its water of hydration. An intrinsic equilibrium constant, valid across a range of background electrolyte concentrations, is the primary advantage of the TLM over the CCM.

Bloesch et al. (1987) were successful in modeling B adsorption on goethite using the Stern model interpretation of Bowden et al. (1977). These researchers assumed that B could adsorb as one of four solution B species including:  $B(OH)_4^-$ ,  $B_3O_3(OH)_4^-$ ,  $B_4O_5(OH)_4^{2-}$ , and  $B_5O_6(OH)_4^-$ , but was adsorbed predominantly as  $B(OH)_4^-$ . The adsorption of  $B(OH)_3$  was not considered.

The kinetics of B reactions in soils have not been extensively studied. Most of the kinetic information currently available pertains to B desorption and release (Griffin and Burau, 1974; Peryea et al., 1985a,b). No reaction mechanisms were established as a result of these studies, as desorption and dissolution were suggested as possible causes of B release. What is particularly lacking is kinetic information pertaining to B reactions with sesquioxide materials, which in many instances, are the soil components most reactive with B.

The few kinetic studies published thus far that report rate information pertaining to B adsorption phenomena have utilized methods that measure relatively slow processes (Griffin and Burau, 1974; Peryea et al., 1985a,b; Sharma et al., 1989). The fact that several different kinetic models will fit a given set of adsorption data (Sharma et al., 1989) indicates that the kinetic measurements thus far obtained may not pertain to the chemical kinetics of B adsorption and desorption. This is perhaps a consequence of the batch and flow methodologies used in these studies. It is likely that the reaction step whereby B solution species bond to surface sites of soil colloids is far too rapid to be monitored by these kinetic techniques. Surface complexation reactions involving ligand exchange are typically very rapid, with reaction times of a few seconds or less (Sparks, 1989). A rapid kinetic technique, such as the pressure-jump method, must be used if the rates of chemical reaction in the overall adsorption process are to be measured, thus revealing the mechanism of reaction (Sparks and Zhang, 1991).

Chemical relaxation kinetic studies of B reactions have been limited to investigations of polymerization reactions in aqueous  $B(OH)_3$  solutions as well as B complexation reactions with organics (Pizer and Babcock, 1977). Osugi et al. (1968) used pressure-jump spectrometry to determine the forward and reverse rate constants for the formation of the trimeric B solution species  $B_3O_3(OH)_4^-$ , postulated by Ingri (1962). Anderson et al. (1964), using the temperature-jump technique, determined the rate constants associated with this same polymerization reaction, as well as for the formation of a pentamer,  $B_5O_6(OH)_4^-$ . The rate constants for the trimer polymerization reaction were in substantial agreement with those obtained by Osugi et al. (1968).

In this study, the pressure-jump relaxation method was used to determine the chemical reaction rates of B adsorption processes on alumina ( $\gamma-Al_2O_3$ ). This rate

information was then analyzed to establish the mechanisms of B adsorption and desorption. Such information is needed to accurately predict the ultimate fate and availability of soil B. Additionally, four surface complexation models were tested for their ability to describe both adsorption isotherm and pressure-jump relaxation rate data. None of these models, the CCM (Stumm et al., 1980), the DLM (Stumm et al., 1970), the MSM of Bowden et al. (1977), or the TLM (Hayes and Leckie, 1987), have distinguished themselves as most appropriate for modeling of surface complexation phenomena based on equilibrium considerations alone. The four EDL models were evaluated for their ability to predict the effects of surface potential on both the equilibrium positioning and reaction rates of B adsorption.

## MATERIALS AND METHODS

### Aluminum Oxide Characterization and Static Measurements

Aluminum Oxide C, a manufactured alumina (Degussa Corp., Teterboro, NJ) was used as the adsorbent for all phases of the static and kinetic studies of B adsorption. Although not a common soil mineral, alumina has been widely used as a soil oxide analog and its chemical and physical properties are well documented due to its extensive applications as a chemical catalyst. It has been perhaps the most frequently used adsorbent in past chemical relaxation studies of colloidal suspensions (Sparks, 1989; Yasunaga and Ikeda, 1986). Its electrochemical surface properties are similar to naturally occurring soil oxides, yet its uniform composition lends itself to interpretation of complex adsorption processes occurring on its surface. The pertinent physical and chemical properties of the alumina were determined prior to collection of chemical relaxation data and are elaborated below.

All reagents were analytical grade and used without further purification. Polyethylene containers were used for storage and analysis of all suspensions and solutions throughout the entire study to avoid B or silicate contamination from borosilicate glassware.

An alumina stock suspension in deionized  $H_2O$  was prepared and used in both the static and kinetic studies. The stock suspension was dialyzed repeatedly to remove entrained electrolytes until the conductivity of the dialyzate was nearly equal ( $\pm 1 \mu S cm^{-1}$ ) to that of deionized  $H_2O$  ( $0.9 \pm 0.1 \mu S cm^{-1}$ ) after a 24-h period. Goldberg and Glaubig (1988) recommend washing alumina to remove soluble surface layers prior to its use in adsorption studies. The final concentration of the stock alumina suspension after dialysis was determined gravimetrically by drying a known volume of the stock suspension at 378 K.

The specific surface area of the alumina is supplied by the manufacturer without further treatment and after the dialysis treatment was determined by the EGME method (Heilman et al., 1965). Specific surface area measurements using the BET- $N_2$  gas adsorption method were also supplied by the manufacturer ( $100 \pm 15 m^2 g^{-1}$ ). The EGME specific surface area measurements ( $75 \pm 16 m^2 g^{-1}$  for unwashed alumina) were not significantly different from the BET- $N_2$  values. Dialysis had no significant effect on the specific surface area of the alumina ( $76.1 \pm 1.3 m^2 g^{-1}$  for dialyzed alumina).

Surface acidity constants were determined by potentiometric titration of the alumina suspensions ( $13.1 g L^{-1}$ ) with NaOH and HCl in 0.0001, 0.01, and 0.5 mol  $L^{-1}$   $NaNO_3$ . The pH of the suspension was monitored throughout the titration using a Radiometer PHM 82 pH meter equipped with a Radiometer

GK2401B combination electrode (Radiometer Copenhagen, Denmark). A nonlinear least-squares optimization procedure (FITEQL Version 2.0, Westall, 1982) was used to model the titration data and determine the first and second acid dissociation constants ( $K_1^{\text{int}}$  and  $K_2^{\text{int}}$ , respectively) and surface site density for the alumina surface (Table 1). The FITEQL program provides four EDL model options for modeling of surface acidity and adsorption phenomena: the CCM (Stumm et al., 1980), the DLM (Stumm et al., 1970), the MSM (Bowden et al., 1977), and the TLM (Hayes and Leckie, 1987). The surface acidity constants and site density were determined using each of the four models, as all four FITEQL models were subsequently tested for their ability to simulate the B adsorption data (Table 1). The values of  $K_1^{\text{int}}$ ,  $K_2^{\text{int}}$ , and the site density as determined from a given EDL model, were held constant in optimizing the equilibrium constants for B adsorption using the same model. Equilibrium constants for the outer sphere adsorption of  $\text{Na}^+$  and  $\text{NO}_3^-$  ( $K_{\text{Na}}^{\text{int}}$  and  $K_{\text{NO}_3}^{\text{int}}$ , respectively), which are also required for the TLM, were obtained from the literature (Westall, 1982) (Table 1). The two capacitance values required for the TLM, the inner capacitance between  $\alpha$  and  $\beta$  layers ( $C_1$ ) and the outer capacitance between the  $\beta$  layer and the diffuse layer ( $C_2$ ), were also obtained from the literature (Westall, 1982), as were the single inner capacitances used when testing the CCM (Goldberg and Glaubig, 1985) and the MSM (Westall, 1982) (Table 1). These same capacitance values were also used when modeling the B adsorption data using these three EDL models.

The mass law expressions describing the surface acidity and electrolyte adsorption reactions are

$$K_+^{\text{int}} = \frac{[\text{AlOH}][\text{H}^+]}{[\text{AlOH}_2^+]} \exp(-F\psi_\alpha/RT) \quad [1]$$

$$K_-^{\text{int}} = \frac{[\text{AlO}^-][\text{H}^+]}{[\text{AlOH}]} \exp(-F\psi_\alpha/RT) \quad [2]$$

$$K_{\text{NO}_3}^{\text{int}} = \frac{[\text{AlOH}_2^+ - \text{NO}_3^-]}{[\text{AlOH}_2^+][\text{NO}_3^-]} \exp(-\psi_\beta F/RT) \quad [3]$$

$$K_{\text{Na}}^{\text{int}} = \frac{[\text{AlO}^- - \text{Na}^+]}{[\text{AlO}^-][\text{Na}^+]} \exp(\psi_\beta F/RT) \quad [4]$$

where  $F$  is the Faraday constant. The exponential terms represent surface activity coefficients for a charged surface and the brackets denote concentrations ( $\text{mol L}^{-1}$ ). The terms  $\psi_\alpha$  and  $\psi_\beta$  represent the electrical potentials at the  $\alpha$  and  $\beta$  layers, respectively.

Boron adsorption was measured across the pH range of 7.0

**Table 1. Electric double layer model parameters for alumina surface acidity reactions used in the four FITEQL model options.**

Model	$-\log K_1^{\text{int}}$	$-\log K_2^{\text{int}}$	Capacitance†	$\log K_{\text{Na}}^{\text{int}}$ or $\log K_{\text{NO}_3}^{\text{int}}$	Site density
			$\text{F m}^{-2}$		$\text{nm}^{-2}$
Constant capacitance	6.7	9.0	$C_1 = 1.06\ddagger$	NA§	1.3
Diffuse layer	7.3	8.6	NA	NA	0.9
Modified stern	7.3	8.5	$C_1 = 2.40\¶$	NA	0.9
Triple layer	7.0	8.8	$C_1 = 1.2$ $C_2 = 0.2$	$\log K_{\text{Na}}^{\text{int}} = -8.3$ $\log K_{\text{NO}_3}^{\text{int}} = 8.3$	0.9

†  $C_1$  = inner layer capacitance;  $C_2$  = outer layer capacitance.

‡ From Goldberg and Glaubig (1985).

§ Not applicable.

¶ From Westall (1982).

#  $C_1$ ,  $C_2$ ,  $\log K_{\text{Na}}^{\text{int}}$ , and  $\log K_{\text{NO}_3}^{\text{int}}$  from Westall (1982).

to 10.8 in  $35 \text{ g L}^{-1}$  alumina suspensions. The pH of the suspensions was adjusted with additions of either  $\text{HNO}_3$  or  $\text{NaOH}$ . Boron was added to the alumina suspensions as  $\text{B}(\text{OH})_3$ . Total B in the suspensions was held constant at  $0.012 \text{ mol L}^{-1}$ . Boron speciation as  $\text{B}(\text{OH})_3$  and  $\text{B}(\text{OH})_4^-$  was controlled by changing the pH of the suspensions. Total B adsorbed was assumed to be the difference between initial total B added and that remaining in the suspension supernatant after a 2-h equilibration period. The 2-h equilibration period was chosen to avoid dissolution of the adsorbent phase resulting from pH adjustment of the suspensions (Goldberg and Glaubig, 1988). The sample suspensions were equilibrated on a reciprocal shaker at low speed. The supernatant was obtained by high-speed centrifugation at  $34\,500 \text{ g}$  for 30 min (Sorvall RC-5B, DuPont Instruments, Newtown, CT), followed by filtration through a  $0.2\text{-}\mu\text{m}$  membrane filter (Gelman Sciences, Ann Arbor, MI). Aluminum remaining in the supernatant was measured by inductively coupled plasma-atomic emission spectrometry. Removal of Al from the supernatant following centrifugation and filtration was  $\geq 99.99\%$  for all suspensions throughout the pH range of the study. Total B remaining in the supernatant was determined by the azomethine-H photocolometry method (Parker and Gardner, 1981) at 420 nm with a Hewlett Packard 8452A diode array spectrophotometer (Hewlett Packard Co., Palo Alto, CA). Boron speciation in the equilibrium supernatant was predicted using the formation constant for  $\text{B}(\text{OH})_4^-$  calculated as a function of temperature and ionic strength (Mesmer et al., 1972) assuming no aqueous polyborates were formed (Ingri, 1962).

Boron adsorption data were modeled using each of the four FITEQL EDL models assuming either  $\text{B}(\text{OH})_3$ ,  $\text{B}(\text{OH})_4^-$ , or both  $\text{B}(\text{OH})_3$  and  $\text{B}(\text{OH})_4^-$  could be adsorbed. Depending on the assumptions inherent in each of the models, the data were also modeled assuming B could be adsorbed as an outer sphere or inner sphere complex. The FITEQL program was then used to determine intrinsic equilibrium constants for the various adsorbed B species. In addition to optimized adsorption constants, the program output also included the equilibrium concentrations of all defined chemical species for each datum point of the adsorption isotherm, both on the alumina surface and in the supernatant. The equilibrium information provided was dependent on both the reaction mechanism proposed and the model used. For instance, the CCM does not take into account adsorption of background electrolyte ions or allow for the assumption of outer sphere adsorption. Information regarding the concentrations of solution and adsorbed background electrolyte as well as outer sphere adsorbed B species is therefore not provided as output from this model.

The FITEQL program (Westall, 1982) also provides a goodness-of-fit parameter ( $V$ ) as output for each model, which is defined as

$$V = \frac{\sum (Y_i/s_i)^2}{(N_p N_c) - N_a} \quad [5]$$

where  $Y_i$  is the residual for each isotherm data point  $i$ ,  $s_i$  is the error estimate,  $N_p$  is the number of isotherm data points,  $N_c$  is the number of components for which both total and free concentrations are known, and  $N_a$  is the number of adjustable parameters (Hayes et al., 1991). This parameter was used in comparing the quality of fit of each EDL model to the B adsorption isotherm data. Error estimates used for all EDL models and all isotherm data points were 0.01 and 0.00001  $\text{mol L}^{-1}$  relative and absolute errors, respectively, for total B, and 0.02303 and 0.0  $\text{mol L}^{-1}$  relative and absolute errors, respectively, for free  $\text{H}^+$  concentrations.

## Pressure-Jump Relaxation Measurements

The rate constants associated with adsorption and desorption reactions of B solution species on  $\gamma$ - $\text{Al}_2\text{O}_3$  surfaces were determined by analysis of the dependence of pressure-jump relaxation times ( $\tau$ ) on proposed reactant species concentrations, based on a particular assumed reaction mechanism. This procedure was also used to test the validity of the various possible reaction mechanisms that could account for the removal of B species from solution in oxide suspensions.

Relaxation spectra in response to a pressure perturbation were sought in aqueous alumina suspensions with  $0.012 \text{ mol B L}^{-1}$  at various ionic strengths up to  $0.1 \text{ mol L}^{-1}$ . A 0.05-mm-thick brass foil was used to seal the autoclave, producing a pressure drop of 13.2 MPa following bursting. Relaxations were induced, detected, and recorded using a DIA-RPC P-jump autoclave in combination with a DIA-RPM Wheatstone bridge, and DIA-RRC analog-to-digital converter (Dia-log Co., Düsseldorf, Germany), respectively. An AIM-65 computer (Rockwell International, Anaheim, CA) was used to calculate  $\tau$  from the relaxation curves and provide statistical parameters regarding  $\tau$  measurement precision. Relaxation curves were displayed on a Kenwood CS-1021 oscilloscope (Kenwood, Japan) for visual inspection.

Maximum concentrations of  $0.012 \text{ mol total B L}^{-1}$  were used to avoid formation of aqueous B polymer species (Ingri, 1962), which might also undergo adsorption reactions (Keren and Bingham, 1985). An iterative procedure was used to calculate the portion of total B as  $\text{B(OH)}_4^-$  in each sample, as dictated by the pH, to account for the contribution of  $\text{B(OH)}_4^-$  to the ionic strength of the supernatant. The amount of  $\text{NaNO}_3$  needed to bring the ionic strength to the desired level was then added. Preliminary studies of the aqueous B-alumina suspensions with ionic strength adjusted to  $0.01 \text{ mol L}^{-1}$  indicated a chemical relaxation effect in response to a pressure drop from pH 7 to 10. All other components of the pressure-jump sample suspensions were tested in all possible combinations to ensure that the relaxations were detected only when alumina and B were both present in the suspensions.

These same suspensions were tested for their stability by placing them in the pressure-jump cell and balancing the Wheatstone bridge with an appropriate electrolyte solution in the reference cell. The stability of the balanced signal from the bridge was then observed and found to be essentially stable for a period of 1 h or more, indicating equilibrium and insignificant particle settling occurred.

Portions of the pressure-jump samples used for  $\tau$  determinations were set aside for subsequent equilibrium reactant concentration measurements. Relaxation times for a series of  $\text{B(OH)}_3$ - $\text{B(OH)}_4^-$ -alumina suspensions of constant total B ( $0.012 \text{ mol L}^{-1}$ ) were obtained from pH 7.3 to 9.7. By changing the pH, the concentrations of the various possible reactants,  $\text{B(OH)}_3$ ,  $\text{B(OH)}_4^-$ , and the negatively charged ( $\text{AlO}^-$ ), neutral ( $\text{AlOH}$ ), and positively charged ( $\text{AlOH}_2^+$ ) alumina surface sites were varied. Several relaxation signals were averaged for each sample ( $\geq 5$  relaxation curves) to enhance the signal-to-noise ratio for each relaxation time measurement. The recording of relaxations following placement of each sample in the pressure-jump cell was limited to a period of not more than 1 h to avoid changes in  $\tau$  due to particle settling.

### Analysis of Relaxation Times and Electrical Double Layer Model Evaluation

Equilibrium determinations for  $\tau$  analysis consisted of measuring the pH of the sample suspension and total B remaining in solution following adsorption. Total B was determined by the

azomethine-H colorimetric method given above. The amount of  $\text{B(OH)}_3$  and  $\text{B(OH)}_4^-$  remaining in the suspension supernatant was then calculated based on the conditional equilibrium constant for the  $\text{B(OH)}_3/\text{B(OH)}_4^-$  equilibrium ( $\log K = 9.15$ ) (Mesmer et al., 1972), the amount of total B, and the pH. Total B remaining in the supernatant, free  $\text{B(OH)}_4^-$ , and pH at equilibrium were then used as input for the FITEQL equilibrium speciation program.

Output obtained from the FITEQL program included all concentrations of model-defined adsorbed and aqueous species. These included: the proposed adsorbed B species for a given reaction mechanism tested, outer sphere background electrolyte surface complexes (if applicable to the model), and the concentrations of the remaining free pH-dependent surface sites. The electrical potential at the various planes of adsorption pertinent to each model tested were also provided based on the previously determined surface acidity constants and the calculated surface charge.

Using the equilibrium output obtained for each model and mechanism tested, the  $\tau$  dependence on the concentrations of the various reactants for a particular assumed reaction mechanism was then tested. The influence of the surface potential on the extent and rate of B adsorption at the assumed plane of adsorption was also accounted for in testing each reaction mechanism.

Rate constants for the adsorption of B species were obtained by a graphical analysis stemming from the derived dependence of  $\tau$  on the proposed reactant species concentrations. The relationship between the rate constants and  $\tau$  varies with the particular reaction mechanism assumed.

Once conformity of relaxation data to a proposed reaction mechanism was found, agreement between an intrinsic equilibrium constant obtained from static measurements and a kinetic equilibrium constant obtained from the ratio  $k_i^m/k_r^m$  was tested. Such agreement between equilibrium- and kinetic-derived constants was considered validation of the reaction mechanism.

## RESULTS AND DISCUSSION

### Static Measurements

Boron adsorption in alumina suspensions ( $0.012 \text{ mol L}^{-1}$  total B) increased as pH increased from 7.0 to 8.5, then decreased as pH increased to 10.8 (Fig. 1). This trend was also found for B adsorption on clays and oxide surfaces by others (Hingston, 1964; Sims and Bingham, 1968a). Goldberg and Glaubig (1985) studied B adsorption on several Al oxides and found that B adsorption was greatly affected by pH, exhibiting sharp maxima near pH 6 to 7. Boron adsorption on alumina ( $\gamma$ - $\text{Al}_2\text{O}_3$ ) was the exception, however, exhibiting a flattened adsorption envelope with a more gradual response to changes in pH. Maximum B adsorption occurred across a broad range of pH 5 to 8. A similar broad adsorption envelope was obtained in this study for B adsorption on alumina (Fig. 1).

Modeling of the B adsorption data yielded varying results depending on the model chosen and the B species assumed to be adsorbed. All four models included in the FITEQL program adequately simulated the B adsorption behavior across the pH range tested. As modeling of the B adsorption data using the four EDL models was central to the objectives of the pressure-jump investigation, these results will be discussed below within the context of interpreting the pressure-jump results.

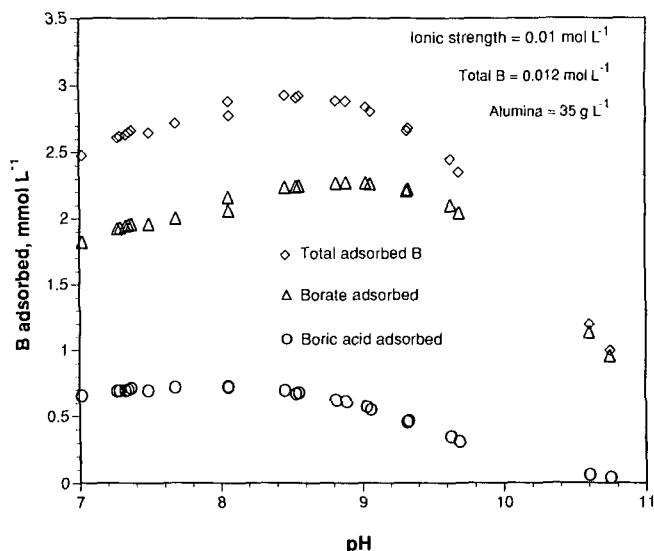


Fig. 1. Adsorption of  $B(OH)_3$  and  $B(OH)_4^-$ , and total adsorption of B on alumina, as a function of pH. Boric acid and  $B(OH)_4^-$  adsorption were modeled using the triple layer model assuming inner sphere adsorption.

Alumina suspensions ( $35 \text{ g L}^{-1}$ ) with  $0.012 \text{ mol L}^{-1}$  total B and ionic strength maintained at  $0.01 \text{ mol L}^{-1}$  remained unflocculated for a minimum of 1 h. All pressure-jump samples were subsequently adjusted to  $0.01 \text{ mol L}^{-1}$  ionic strength with  $\text{NaNO}_3$  as the background electrolyte.

### Pressure-Jump Measurements

Pressure-jump relaxations were detected in alumina- $B(OH)_3$  suspensions from pH 7.3 to 9.7, within a time region of 1.6 s. These same relaxations were not detected in solutions or suspensions containing the various other components of the B-alumina suspensions unless both alumina and B were present. This indicated that the relaxation spectrum was due to an interaction between B and alumina. No additional relaxations were detected in the B-alumina suspensions within 1.75 min.

Relaxation times for pressure-jump samples with equal particle and total B concentrations decreased as pH increased, indicating that the detected relaxation was due to one or more of the pH-dependent surface or solution species present in the suspension. Since  $\tau$  is related to the forward and reverse rate constants governing the reaction, a smaller  $\tau$  indicates the equilibration is occurring at a more rapid rate. Although the rate constants remain unchanged, the rate of the forward reaction will increase as the concentration of the reactants increases.

The relationship between  $\tau$  and the amount of free  $B(OH)_4^-$  in solution is shown in Fig. 2. The relaxation time decreased with an increase in  $B(OH)_4^-$  in the suspension, indicating that the relaxation could be attributable to  $B(OH)_4^-$  adsorption reactions.

### Triple Layer Model Application to Boron Adsorption Isotherm Data

Since the intrinsic rate and equilibrium constants for the adsorption reaction are dependent on the activity of

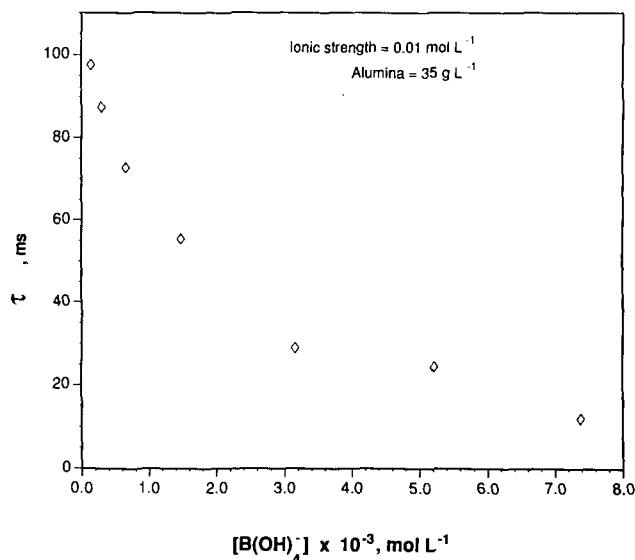


Fig. 2. The effect of  $B(OH)_4^-$  concentration on relaxation times ( $\tau$ ) measured in alumina suspensions with  $0.012 \text{ mol L}^{-1}$  total B.

the adsorptive in the EDL surrounding the adsorbate particles and not on their concentrations in the bulk solution per se, the effect of the electrical potential at the plane of adsorption on the adsorptive activity must be considered.

The mechanisms proposed for B adsorption on the alumina surface were tested under the following assumptions. Several researchers have suggested that B can be adsorbed from solution as both the neutral  $B(OH)_3$  and  $B(OH)_4^-$  species (Hingston, 1964; Keren et al., 1981) and possibly as one or more of several polyborate species (Keren and Bingham, 1985). In designing the experiments, total B concentrations were kept below levels that would promote the formation of aqueous polyborates, therefore the latter possibility could be ignored. It was then assumed that B could be adsorbed as  $B(OH)_3$ ,  $B(OH)_4^-$ , or both. The first criterion for (EDL) model validity was the ability to simulate the B adsorption data. If the model was successful in this capacity, it was then tested for its ability to fit the kinetic data.

Because pressure-jump with conductivity detection can only be used to monitor reactions that involve a change in concentration of ionic species, the adsorption of neutral  $B(OH)_3$  molecules can only be detected if it results in the desorption of an ionic product, such as a hydronium ion or hydroxyl ion. Convergence of the FITEQL equilibrium speciation program for the TLM-IS was not obtained when modeling the  $B(OH)_3$  adsorption reaction with the appropriate stoichiometry that would yield either of these two ionic product species.

The adsorption of  $B(OH)_3$  on a neutral  $\text{AlOH}$  site would require that the leaving group be  $\text{H}_2\text{O}$ . Since all reactants and products in this reaction scheme are unchanged, no change in conductivity would result from this adsorption reaction. Therefore, the relaxation effect could not be attributed to this process. Nonetheless, an attempt was made to model this B adsorption reaction mechanism using the TLM-IS but the attempt was unsuccess-

cessful when it was assumed that  $B(OH)_3$  was the only species adsorbed.

Although the relaxation in B-alumina suspensions cannot be attributed to  $B(OH)_3$  adsorption, and  $B(OH)_3$  adsorption could not account for all adsorbed B in the pressure-jump suspensions, this reaction may occur concurrently with  $B(OH)_4^-$  adsorption. Modeling of the B adsorption isotherm data using the TLM-IS was successful under the assumption of  $B(OH)_3$  adsorption on a neutral AlOH site when it was assumed that  $B(OH)_4^-$  was also competitively adsorbed on a neutral site (Fig. 1).

Convergence of the FITEQL equilibrium speciation program for the TLM-IS was not obtained using the B adsorption isotherm data when assuming  $B(OH)_4^-$  was the adsorptive and either  $AlOH_2^+$  or  $AlO^-$  was the reactant surface functional group, nor was convergence obtained with  $B(OH)_4^-$  as the lone adsorptive and AlOH as the reactant site. The TLM-IS was only successful in modeling  $B(OH)_4^-$  adsorption when it was assumed that both the neutral  $B(OH)_3$  species as well as the anionic  $B(OH)_4^-$  species were adsorbed at neutral AlOH sites, resulting in a neutral and negatively charged adsorbed-B site, respectively. In each reaction scheme,  $H_2O$  is the leaving group. Throughout the pH range studied, the amount of  $B(OH)_4^-$  adsorbed was more than three times the amount of  $B(OH)_3$  adsorbed as simulated by the TLM-IS using the FITEQL program (Fig. 1). This reaction scheme for B adsorption is consistent with the observation that B adsorbs regardless of the overall charge on the surface of the oxide and that it adsorbs across a wide range of pH. The adsorption of  $B(OH)_3$  ( $pK_a = 9.3$  for  $B(OH)_3-B(OH)_4^-$  hydrolysis reaction) would occur at  $pH < 10$  provided neutral AlOH surface groups remain available. However, under increasingly acidic conditions ( $pH < 5$ ), protonation of the neutral AlOH site and formation of the  $AlOH_2^+$  surface group decreases the number of sites favorable for B adsorption. As pH increases above 7, and  $B(OH)_4^-$  solution species becomes more prevalent and total B adsorption increases. At  $pH > 10$ , deprotonation of the neutral surface site and formation of the  $AlO^-$  site reduces the number of sites available for B adsorption.

### Analysis of Relaxation Data Using the Triple Layer Model-Inner-Sphere Adsorption

Since only the  $B(OH)_3$  and  $B(OH)_4^-$  adsorption reactions involving the neutral surface site could be modeled successfully with the TLM-IS, and only the adsorption of  $B(OH)_4^-$  would result in a change in conductivity, the correlation between pressure-jump relaxation times and the  $B(OH)_4^-$  adsorption reaction mechanism was tested using the FITEQL equilibrium output.

The reaction mechanism for the adsorption of  $B(OH)_4^-$  on a neutral AlOH surface group, involving two reactants and two products, of which one of the products,  $H_2O$ , is quasi-constant, can be written as



The symbol  $AlOB(OH)_3^-$  represents the  $B(OH)_4^-$  inner sphere adsorption complex on the alumina surface, and

the minus sign denotes that adsorption of the  $B(OH)_4^-$  anion imparts a negative charge to the surface. The mass law expression for Eq. [6] is

$$K_{BIS} = \frac{[AlOB(OH)_3^-][H_2O]}{[AlOH][B(OH)_4^-]} \quad [7]$$

The terms in brackets denote concentrations of neutral surface sites,  $B(OH)_4^-$ ,  $AlOB(OH)_3^-$ , and  $H_2O$ , and  $K_{BIS}$  is the conditional equilibrium constant for the reaction.

From chemical relaxation theory (Bernasconi, 1976), for a reaction mechanism of this form, the dependence of the reciprocal of the relaxation time ( $\tau^{-1}$ ) on the reactant concentrations is given by

$$\tau^{-1} = k_f \{ [AlOH] + [B(OH)_4^-] \} + k_r [H_2O] \quad [8]$$

where  $k_f$  is the conditional forward rate constant and  $k_r$  is the conditional reverse rate constant. The relationship between the conditional  $k_f$  and  $k_r$  and the intrinsic  $k_f^{int}$  and  $k_r^{int}$  can be derived as follows.

From chemical kinetics,

$$K_{BIS} = k_f/k_r \quad [9]$$

The intrinsic equilibrium constant for  $B(OH)_4^-$  inner sphere adsorption ( $K_{BIS}^{int}$ ) is related to  $K_{BIS}$  by

$$K_{BIS}^{int} = K_{BIS} \exp\left(\frac{-\psi_a F}{RT}\right) \quad [10]$$

where  $\psi_a$  is the surface potential at the plane of inner sphere adsorption. Combining Eq. [9] and [10] leads to

$$K_{BIS}^{int} = \frac{k_f^{int}}{k_r^{int}} = \frac{k_f}{k_r} \exp\left(\frac{-\psi_a F}{RT}\right) \quad [11]$$

For the condition of a small perturbation following a sudden pressure drop,  $\psi_a$  remains essentially constant and the activation potentials for the forward and reverse processes are equal and opposite in sign (Hayes and Lackie, 1986). Therefore,

$$K_{BIS}^{int} = \frac{k_f \exp(-\psi_a F/2RT)}{k_r \exp(\psi_a F/2RT)} \quad [12]$$

Combining Eq. [11] and [12] yields

$$k_f = k_f^{int} \exp(\psi_a F/2RT) \quad [13]$$

and

$$k_r = k_r^{int} \exp(-\psi_a F/2RT) \quad [14]$$

Combining Eq. [8], [13], and [14] yields

$$\tau^{-1} = k_f^{int} \exp(\psi_a F/2RT) \{ [AlOH] + [B(OH)_4^-] \} + k_r^{int} \exp(-\psi_a F/2RT) [H_2O] \quad [15]$$

Rearrangement of Eq. [15] leads to

$$\tau^{-1} \exp(\psi_a F/2RT) = k_f^{int} \exp(\psi_a F/RT) \{ [AlOH] + [B(OH)_4^-] \} + k_r^{int} [H_2O] \quad [16]$$

or

$$T_x = k_f^{int} P + k_r^{int} [H_2O] \quad [17]$$

where

$$P = \exp(\psi_a F/RT) \{[AlOH] + [B(OH)_4^-]\} \quad [18]$$

and

$$T_x = \tau^{-1} \exp(\psi_a F/2RT) \quad [19]$$

Therefore, a plot of  $T_x$  vs.  $P$  in Eq. [17] will yield a linear relationship with a slope,  $k_f^{int}$ , and the intercept equal to the product of  $k_f^{int}$  and the quasi-constant concentration of  $H_2O$ , if the proposed reaction mechanism is valid. By dividing the intercept by the concentration of  $H_2O$  in the suspension ( $55.5 \text{ mol L}^{-1}$ ), the intrinsic rate constant for the desorption process is obtained.

A plot of  $T_x$  vs.  $P$  for the relaxation times measured for B adsorption on alumina results in a linear relationship ( $R^2 = 0.92$ , significant at  $P = 0.05$  level) with a slope equal to  $10^{5.52}$  and an intercept equal to 0.10 (Fig. 3). After division of the intercept by the concentration of  $H_2O$ , the rate constant for the desorption of  $B(OH)_4^-$  from the oxide surface is obtained  $10^{-2.74}$ . The ratio  $k_f^{int}/k_r^{int}$  yields an equilibrium constant obtained through kinetic analysis ( $K_{KN}^{int} = 10^{8.26}$ ). Comparison of intrinsic equilibrium constants for the adsorption of  $B(OH)_4^-$  on the alumina surface from kinetic ( $K_{KN}^{int}$ ) and static analysis using the TLM-IS shows substantial agreement between the two (Table 2). This indicates that the proposed  $B(OH)_4^-$  adsorption reaction mechanism is valid.

### Pressure-Jump Data Analysis Using Other Electrical Double Layer Models

The three other surface complexation model options provided by the FITEQL program, the CCM (Stumm et al., 1980), the DLM (Stumm et al., 1970), and the MSM (Bowden et al., 1977), as well as the TLM assuming outer sphere B adsorption (TLM-OS) (Hayes and Leckie, 1987) were tested for their ability to describe the kinetic data. These models are alike in their inclusion of both mass law and material balance constraints on

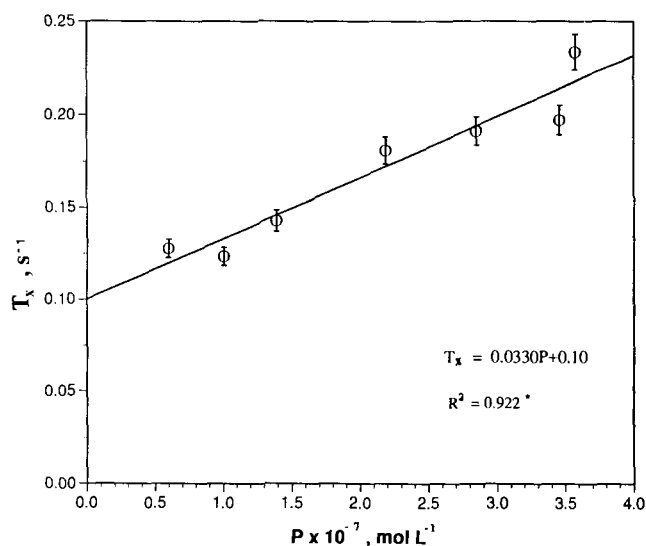


Fig. 3. Plot of  $T_x$  vs.  $P$  in Eq. [17] for the  $B(OH)_4^-$  inner sphere adsorption mechanism using the triple layer model assuming inner sphere adsorption.

equilibrium concentrations but differ in their interpretation of the EDL. These differences include the particular definition of the type of surface complex formed in the adsorption process, the number and location of planes of adsorption, and the equation describing the relationship between surface charge ( $\sigma$ ) and surface potential ( $\psi$ ) at the plane of adsorption (Westall and Hohl, 1980). The models also differ in the number of parameters that are adjustable in fitting the data. All the models mentioned here are adaptations of the original Stern model of the oxide surface-electrolyte solution interface (Westall and Hohl, 1980). The four surface complexation models examined in this study are thoroughly developed, compared, and contrasted in Westall and Hohl (1980) and Goldberg (1992).

In modeling the B adsorption data obtained in this study using the CCM, DLM, MSM, and TLM-IS, the models succeeded only under the assumption that B, either as  $B(OH)_3$  or  $B(OH)_4^-$ , was adsorbed on neutral surface sites of the alumina, and only when  $H_2O$  was assumed to be the leaving ligand in the exchange process. All stoichiometrically feasible reaction mechanisms were tested for each model, including adsorption on negatively charged, neutral, and positively charged surface sites, with  $H^+$ ,  $OH^-$ , and  $H_2O$  as the leaving ligand, as well as mono- and bidentate adsorption. For all of the models used, as in the TLM-IS, the model equilibrium speciation output indicated that B adsorption in the pH range of this study (pH 7–10.75) was predominantly or entirely as  $B(OH)_4^-$ .

The intrinsic equilibrium constant for B adsorption on alumina provided as output from the FITEQL program using the CCM is presented in Table 2. As required by the assumptions inherent in the development of this model, only adsorption in the  $\alpha$  layer is considered.

The CCM was unsuccessful in modeling the B adsorption data when it was assumed that both nonionic  $B(OH)_3$  and the  $B(OH)_4^-$  anion could be adsorbed simultaneously. It successfully simulated the adsorption data when it was assumed that  $B(OH)_4^-$  was the sole adsorptive, however (Table 2).

The model-generated electrical potentials at the plane of adsorption and equilibrium concentrations of the reactant species in the alumina-B suspensions were used in testing the proposed reaction mechanism for B adsorption. The equation describing the relationship between

Table 2. Model-dependent intrinsic equilibrium constants for B adsorption obtained using the FITEQL program.

Model	$B(OH)_4^-$ adsorption constant	$B(OH)_3$ adsorption constant	$V^\dagger$
Triple layer, inner sphere $\ddagger$	7.69	2.16	0.61
Constant capacitance	6.28	NC $\S$	0.94
Diffuse layer $\ddagger$	6.39	1.47	0.93
Modified stern $\ddagger$	12.09	2.24	1.02
Triple layer, outer sphere	12.48	NC $\S$	0.71

$\dagger V = \sum(Y_i/s)^2 / [(N_p N_c) - N_d]$ .

$\ddagger B(OH)_4^-$  adsorption constant was unaffected by inclusion of  $B(OH)_3$  adsorption.

$\S$  No convergence of the FITEQL optimization procedure was obtained with inclusion of  $B(OH)_3$  adsorption.

$\ddagger$  Convergence obtained only with inclusion of  $B(OH)_3$  adsorption.

$\tau$  and the reactant concentrations is the same as for the TLM-IS (Eq. [16]). The plot of  $T_x$  vs.  $P$  in Eq. [17] using the CCM output provided a  $K_{\text{kin}}^{\text{int}}$  value ( $10^{7.34}$ ) that was more than an order of magnitude greater than the static equilibrium constant (Table 2). The coefficient of multiple determination for the plot of Eq. [17] using the CCM indicated a poor correlation between  $\tau$  and the reactant activity terms ( $R^2 = 0.46$ , not significant at  $P > 0.05$  level). Goldberg and Glaubig (1985, 1986) have used the CCM extensively to model B adsorption reactions on various adsorbents. In each case, they assumed neutral  $\text{B(OH)}_3$  adsorption on a neutral surface site with no net change in charge on the alumina surface. The magnitude of the FITEQL equilibrium constant for B adsorption obtained in their studies of various adsorbents was similar to that obtained in this study. Since they assume adsorption of an uncharged solution species in their reaction scheme, however, there is no electrostatic effect on the B adsorption process.

The equilibrium constant for  $\text{B(OH)}_4^-$  adsorption given by the DLM was of similar magnitude to the CCM static equilibrium constant (Table 2). The DLM successfully modeled the B adsorption data assuming either  $\text{B(OH)}_3$  and  $\text{B(OH)}_4^-$  could both be adsorbed or only  $\text{B(OH)}_4^-$  could be adsorbed. The value of the  $\text{B(OH)}_4^-$  adsorption constant was largely unaffected by the assumption of simultaneous  $\text{B(OH)}_3$  adsorption (Table 2).

The relationship between  $\tau$  and the reactant concentrations for the DLM is similar to the TLM-IS and the CCM (Eq. [16]) but different values for  $\psi_\alpha$  and the  $\text{AlOH}$  concentration are generated. Neither DLM assumption [ $\text{B(OH)}_4^-$  adsorption, or  $\text{B(OH)}_4^-$  and  $\text{B(OH)}_3$  adsorption] yielded a rational  $T_x$  vs.  $P$  plot, however, as in either case the intercept was negative, indicating a negative rate constant for the  $\text{B(OH)}_4^-$  desorption process. This was largely due to the value of  $\psi_\alpha$  in the exponential terms in Eq. [16] generated as DLM output. Since  $\psi_\alpha$  has an exponential effect on the values of  $T_x$  and  $P$  in Eq. [17], its influence is much greater than the reactant concentrations themselves. Due to the negative intercept of Eq. [17], no kinetic equilibrium constant was obtainable from the DLM output.

The MSM was successful in modeling B adsorption only when assuming that both  $\text{B(OH)}_3$  and  $\text{B(OH)}_4^-$  were adsorbed (Table 2). The intrinsic equilibrium constant for  $\text{B(OH)}_4^-$  adsorption obtained from the MSM treatment of the isotherm data (Table 2) differs substantially from those obtained from the TLM-IS, DLM, and CCM. The MSM static equilibrium constant for  $\text{B(OH)}_4^-$  adsorption was nearly six orders of magnitude greater than the CCM and DLM constants, and nearly five orders of magnitude greater than the TLM-IS constant. This was a result of the exponential effect of the  $\beta$ -layer potentials predicted by the MSM, which were large ( $-0.5$  to  $-0.6$  V) relative to the  $\alpha$ -layer potentials predicted by the other models ( $-0.1$  to  $-0.3$  V). The potential at the  $\beta$  layer affects  $\text{B(OH)}_4^-$  adsorption in the MSM, since only  $\text{H}^+$  and  $\text{OH}^-$  can enter the  $\alpha$  layer. All other specifically adsorbed ions are assigned to the  $\beta$  layer at some distance from the oxide surface (Westall and Hohl, 1980).

The kinetic test of the model output indicated that the

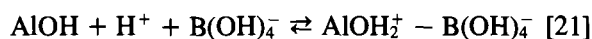
MSM was not an accurate representation of B adsorption at the charged alumina interface, however. The  $\tau$  vs. reactant concentration expression was as in the TLM-IS, CCM, and the DLM (Eq. [16]). However, assuming specific adsorption occurs at the  $\beta$  layer, the MSM-generated values of  $\psi_\beta$  are used instead of  $\psi_\alpha$  in the exponential terms in Eq. [16]. The  $T_x$  vs.  $P$  plot (Eq. [17]) of the MSM output yielded a negative slope, indicating a negative  $k^{\text{int}}$  for  $\text{B(OH)}_4^-$  adsorption. A negative rate constant for the adsorption process is an illogical result, therefore no kinetic equilibrium constant was obtained from the MSM.

The TLM-OS was used in modeling outer sphere complexation of B by the alumina surface as well. The TLM-OS simulated the B adsorption data successfully only when it was assumed that  $\text{B(OH)}_4^-$  was adsorbed electrostatically by a protonated  $\text{AlOH}_2^+$  site (Table 2). Since outer sphere adsorption is considered to be an electrostatic attraction between a charged surface site and an ionic adsorbate, convergence of the FITEQL program was not expected when assuming the neutral  $\text{B(OH)}_3$  species was also adsorbed.

The outer sphere B adsorption mechanism can actually be represented in either of two forms:



where the  $\text{B(OH)}_4^-$  anion is adsorbed at a previously protonated site, or



where the protonation of the surface site and formation of the outer sphere  $\text{B(OH)}_4^-$  surface complex occur simultaneously. The symbol  $\text{AlOH}_2^+ - \text{B(OH)}_4^-$  represents the  $\text{B(OH)}_4^-$  ion-pair complex with the positively charged alumina surface group.

One shortcoming that becomes apparent in using the FITEQL program is its inability to distinguish between single- and multiple-step reactions in model species matrix construction. The FITEQL program is designed such that all chemical species, reactant and product, in the equilibrium chemical system to be modeled are represented as the sum of their components. Species are defined as all of the individual chemical entities to be considered in the chemical equilibrium system of interest, whereas components are defined as those chemical entities whose products make up all the species in the system. No component can be written as a product of a reaction of any of the other components (Westall, 1982). A species can be made up of a single component, however. The end result is that a single reactant species in Eq. [20], the protonated surface site, is codified in the FITEQL species input matrix in the same form as two reactant species in Eq. [21], the neutral surface site and proton. Although the FITEQL model input matrix and model output are identical for each of the rate law expressions (Eq. [20] and [21]), the form of the  $\tau$  vs. reactant concentration expression is different for each reaction mechanism.

For a reaction in which two reactants yield a single product, as in Eq. [20], from chemical relaxation kinetic theory (Bernasconi, 1976), the relationship between  $\tau$  and the reactant concentrations at the final equilibrium is

$$\tau^{-1} = k_{fO2} \{ [\text{AlOH}_2^+] + [\text{B}(\text{OH})_4^-] \} + k_{rO2} \quad [22]$$

where  $k_{fO2}$  is the forward conditional rate constant, and  $k_{rO2}$  is the reverse conditional rate constant for outer sphere  $\text{B}(\text{OH})_4^-$  adsorption according to Eq. [20]. Since it is assumed that  $\text{B}(\text{OH})_4^-$  is adsorbed at the  $\beta$  layer, the intrinsic equilibrium constant for the outer sphere adsorption process ( $K_{\text{BO}2}^{\text{int}}$ ) is given by

$$\begin{aligned} K_{\text{BO}2}^{\text{int}} &= \frac{[\text{AlOH}_2^+ - \text{B}(\text{OH})_4^-]}{[\text{AlOH}_2^+][\text{B}(\text{OH})_4^-]} \exp\left(\frac{-\psi_\beta F}{RT}\right) \\ &= K_{\text{BO}2} \exp\left(\frac{-\psi_\beta F}{RT}\right) \end{aligned} \quad [23]$$

and

$$K_{\text{BO}2} = \frac{k_{fO2}}{k_{rO2}} \quad [24]$$

Therefore,

$$K_{\text{BO}2}^{\text{int}} = \frac{k_{fO2}^{\text{int}}}{k_{rO2}^{\text{int}}} = \frac{k_{fO2}}{k_{rO2}} \exp\left(\frac{-\psi_\beta F}{RT}\right) \quad [25]$$

As in Eq. 12, for a small perturbation, the exponential term in Eq. [25] can be divided between the forward and reverse rate constants such that

$$k_{fO2} = k_{fO2}^{\text{int}} \exp(\psi_\beta F/2RT) \quad [26]$$

and

$$k_{rO2} = k_{rO2}^{\text{int}} \exp(-\psi_\beta F/2RT) \quad [27]$$

Combining Eq. [22], [26], and [27] leads to

$$\begin{aligned} \tau^{-1} &= k_{fO2}^{\text{int}} \exp(\psi_\beta F/2RT) \{ [\text{AlOH}_2^+] + [\text{B}(\text{OH})_4^-] \} \\ &\quad + k_{rO2}^{\text{int}} \exp(-\psi_\beta F/2RT) \end{aligned} \quad [28]$$

Rearrangement of Eq. [28] yields

$$\begin{aligned} \tau^{-1} \exp(\psi_\beta F/2RT) &= k_{fO2}^{\text{int}} \{ \exp(\psi_\beta F/RT) ([\text{AlOH}_2^+] \\ &\quad + [\text{B}(\text{OH})_4^-]) \} + k_{rO2}^{\text{int}} \end{aligned} \quad [29]$$

Therefore, if the two-reactant outer sphere reaction mechanism (Eq. [20]) for B adsorption is valid, a plot of the left-hand side of Eq. [29] vs.  $\exp(\psi_\beta F/RT) ([\text{AlOH}_2^+] + [\text{B}(\text{OH})_4^-])$  will be linear with the slope equal to  $k_{fO2}^{\text{int}}$  and the intercept equal to  $k_{rO2}^{\text{int}}$ .

When plotting the FITEQL output for the TLM-OS according to Eq. [29], a negative intercept was obtained. This indicates a negative reverse rate constant, which is untenable. Therefore no kinetic equilibrium constant was obtained from this exercise.

The form of the  $\tau$  vs. reactant concentration expression for the outer sphere adsorption reaction mechanism as proposed in Eq. [21], involving three reactants and a single product, is unlike that of the two-reactant outer sphere mechanism (Eq. [20]). For a reaction mechanism of this form, the relationship between  $\tau$  and the equilibrium concentrations of the three reactants is given by (Bernasconi, 1976)

$$\begin{aligned} \tau^{-1} &= k_{fO3} ([\text{AlOH}] [\text{B}(\text{OH})_4^-] + [\text{AlOH}][\text{H}^+] \\ &\quad + [\text{H}^+] [\text{B}(\text{OH})_4^-]) + k_{rO3} \end{aligned} \quad [30]$$

where  $k_{fO3}$  is the forward conditional rate constant, and  $k_{rO3}$  is the reverse conditional rate constant for outer sphere  $\text{B}(\text{OH})_4^-$  adsorption according to Eq. [21]. Since the adsorption data were obtained in the region pH 7 to 10.75, the  $\text{H}^+$  concentration was negligible relative to the neutral surface site and  $\text{B}(\text{OH})_4^-$  anion concentrations in the suspensions. The second and third terms enclosed within the parentheses in Eq. [30] can therefore be ignored and Eq. [30] reduces to

$$\tau^{-1} = k_{fO3} ([\text{AlOH}][\text{B}(\text{OH})_4^-]) + k_{rO3} \quad [31]$$

The relationship between the intrinsic and conditional equilibrium constants for  $\text{B}(\text{OH})_4^-$  outer sphere adsorption ( $K_{\text{BO}3}^{\text{int}}$  and  $K_{\text{BO}3}$ , respectively), where two of the reactants are solution species,  $\text{H}^+$ , which must adsorb at the  $\alpha$  layer to form an  $\text{OH}_2^+$  group, and  $\text{B}(\text{OH})_4^-$ , which adsorbs at the  $\beta$  layer, thus becomes

$$K_{\text{BO}3} = \frac{[\text{AlOH}_2^+ - \text{B}(\text{OH})_4^-]}{[\text{AlOH}] [\text{B}(\text{OH})_4^-] [\text{H}^+]} = \frac{k_{fO3}}{k_{rO3}} \quad [32]$$

and

$$K_{\text{BO}3}^{\text{int}} = K_{\text{BO}3} \exp\left(\frac{(\psi_\alpha - \psi_\beta)F}{RT}\right) \quad [33]$$

Therefore,

$$K_{\text{BO}3}^{\text{int}} = \frac{k_{fO3}^{\text{int}}}{k_{rO3}^{\text{int}}} = \frac{k_{fO3}}{k_{rO3}} \exp\left(\frac{(\psi_\alpha - \psi_\beta)F}{RT}\right) \quad [34]$$

For a pressure-jump perturbation of small magnitude

$$k_{fO3}^{\text{int}} = k_{fO3} \exp[(\psi_\alpha - \psi_\beta)F/2RT] \quad [35]$$

and

$$k_{rO3}^{\text{int}} = k_{rO3} \exp[(\psi_\beta - \psi_\alpha)F/2RT] \quad [36]$$

Combining Eq. [31], [35], and [36] yields

$$\begin{aligned} \tau^{-1} &= k_{fO3}^{\text{int}} \exp[(\psi_\beta - \psi_\alpha)F/2RT] ([\text{AlOH}][\text{B}(\text{OH})_4^-]) \\ &\quad + k_{rO3}^{\text{int}} \exp[(\psi_\alpha - \psi_\beta)F/2RT] \end{aligned} \quad [37]$$

which after rearrangement becomes

$$\begin{aligned} \tau^{-1} \exp[(\psi_\beta - \psi_\alpha)F/2RT] &= k_{fO3}^{\text{int}} \exp[(\psi_\beta - \psi_\alpha)F/RT] \\ &\quad ([\text{AlOH}][\text{B}(\text{OH})_4^-]) + k_{rO3}^{\text{int}} \end{aligned} \quad [38]$$

A plot of the left-hand side of Eq. [38] vs. the product of the right-hand exponential term and the reactant concentrations in Eq. [38] will yield a linear relationship if the relaxation measurements pertain to the three-reactant outer sphere adsorption mechanism for  $\text{B}(\text{OH})_4^-$  adsorption.

The coefficient of multiple determination for the plot of Eq. [38] using the TLM-OS for the three-reactant outer sphere reaction mechanism (Eq. [21]) indicated a strong correlation between  $\tau$  and the reactant activity terms ( $R^2 = 0.98$ , significant at  $P = 0.05$  level). However, the  $K_{\text{BIN}}^{\text{int}}$  obtained from the ratio of the slope ( $k_{fO3}^{\text{int}} = 10^{7.35}$ ) and intercept ( $k_{rO3}^{\text{int}} = 10^{0.464}$ ) of the plot of Eq. [38] yields  $K_{\text{BIN}}^{\text{int}} = 10^{6.89}$ . The equilibrium constant obtained from the FITEQL program using the TLM-OS differs from the  $K_{\text{BIN}}^{\text{int}}$  obtained from Eq. [38] by six orders of magnitude (Table 2), indicating the chemical relaxation detected in the B-alumina suspensions is not

attributable to outer sphere adsorption of  $B(OH)_4^-$  at the  $\beta$  layer of the alumina surface.

There is little difference between the CCM, DLM, MSM, TLM-IS, and TLM-OS in their ability to stimulate B adsorption on alumina, despite having dissimilar descriptions of the charged colloid-solution interface. Westall and Hohl (1980) concluded that these same EDL models were all equally suitable for modeling surface acidity using potentiometric titration data. Since all are equally capable of simulating equilibrium data, none of the models yields an unambiguous description of the adsorption energies and electrostatic potentials at the oxide surface, based on equilibrium measurements alone.

Since the electrostatic properties of the surface affect not only the equilibrium positioning of reactions involving charged adsorptives, but also the kinetics of these reactions, a more stringent test of model validity then becomes which model can best fit both static and kinetic data.

Only the TLM-IS was successful in fitting both static and kinetic data for the adsorption of B on alumina. This indicates that the TLM-IS provides the most accurate description of the interaction between adsorbed  $B(OH)_4^-$  and the adsorbent at the colloid-solution interface of the four EDL models tested in this study. The static and pressure-jump relaxation kinetic results using the TLM-IS FITEQL model output indicates that  $B(OH)_4^-$  adsorbs by ligand exchange with neutral OH sites on the alumina surface, with  $H_2O$  as the leaving ligand.

## REFERENCES

- Anderson, J.L., E.M. Eyring, and M.P. Whittaker. 1964. Temperature jump rate studies of polyborate formation in aqueous boric acid. *J. Phys. Chem.* 68:1128-1132.
- Bernasconi, C.F. 1976. Relaxation kinetics. Academic Press, New York.
- Bingham, F.T., A.L. Page, N.T. Coleman, and K. Flach. 1971. Boron adsorption characteristics of selected amorphous soils from Mexico and Hawaii. *Soil Sci. Soc. Am. Proc.* 35:546-550.
- Bloesch, P.M., L.C. Bell, and J.D. Hughes. 1987. Adsorption and desorption of boron by goethite. *Aust. J. Soil Res.* 25:377-390.
- Bowden, J.W., A.M. Posner, and J.P. Quirk. 1977. Ionic adsorption on variable charge mineral surfaces. Theoretical-charge development and titration curves. *Aust. J. Soil Res.* 15:121-136.
- Goldberg, S. 1992. Use of surface complexation models in soil chemical systems. *Adv. Agron.* 47:233-329.
- Goldberg, S., and H.S. Forster. 1991. Boron sorption on calcareous soils and reference calcites. *Soil Sci.* 152:304-310.
- Goldberg, S., and R.A. Glaubig. 1985. Boron adsorption on aluminum and iron oxide minerals. *Soil Sci. Soc. Am. J.* 49:1374-1379.
- Goldberg, S., and R.A. Glaubig. 1986. Boron adsorption on California soils. *Soil Sci. Soc. Am. J.* 50:1173-1176.
- Goldberg, S., and R.A. Glaubig. 1988. Boron and silicon adsorption on an aluminum oxide. *Soil Sci. Soc. Am. J.* 52:87-91.
- Griffin, R.A., and R.G. Burau. 1974. Kinetic and equilibrium studies of boron desorption from soil. *Soil Sci. Soc. Am. Proc.* 38:892-897.
- Hayes, K.F., and J.O. Leckie. 1986. Mechanism of lead ion adsorption at the goethite-water interface. *ACS Symp. Ser.* 323:114-141.
- Hayes, K.F., and J.O. Leckie. 1987. Modeling ionic strength effects on cation adsorption at hydrous oxide/solution interfaces. *J. Colloid Interface Sci.* 115:564-572.
- Hayes, K.F., G. Redden, W. Ela, and J.O. Leckie. 1991. Surface complexation models: An evaluation of model parameter estimation using FITEQL and oxide mineral titration data. *J. Colloid Interface Sci.* 142:448-469.
- Heilman, M.D., D.L. Carter, and C.L. Gonzalez. 1965. The ethylene glycol monoethyl ether (EGME) technique for determining soil-surface area. *Soil Sci.* 100:409-413.
- Hingston, F.J. 1964. Reactions between boron and clays. *Aust. J. Soil Res.* 2:83-95.
- Hingston, F.J., A.M. Posner, and J.P. Quirk. 1972. Anion adsorption by goethite and gibbsite: I. The role of the proton in determining adsorption envelopes. *J. Soil Sci.* 23:177-192.
- Ingri, N. 1962. Equilibrium studies of polyanions: VIII. On the first equilibrium steps in the hydrolysis of boric acid, a comparison between equilibria in 0.1 M and 3.0 M  $NaClO_4$ . *Acta Chem. Scand.* 16:439-448.
- Keren, R., and F.T. Bingham. 1985. Boron in water, soils, and plants. *Adv. Soil Sci.* 1:229-276.
- Keren, R., R.G. Gast, and B. Bar-Yosef. 1981. pH-dependent boron adsorption by Na-montmorillonite. *Soil Sci. Soc. Am. J.* 45:45-48.
- Mesmer, R.E., C.F. Baes, Jr., and F.H. Sweeton. 1972. Acidity measurements at elevated temperatures. VI. Boric acid equilibria. *Inorg. Chem.* 11:537-543.
- Mezumen, U., and R. Keren. 1981. Boron adsorption by soils using a phenomenological adsorption equation. *Soil Sci. Soc. Am. J.* 45:722-726.
- Osugi, J., M. Sato, and T. Fujii. 1968. Pressure-jump technique applied in study of solutions. *Nippon Kagaku Zasshi* 89:562-565.
- Parker, D.R., and E.H. Gardner. 1981. The determination of hot-water-soluble boron in some acid Oregon soils using a modified azomethine-H procedure. *Commun. Soil Sci. Plant Anal.* 12:1311-1322.
- Peryea, F.J., F.T. Bingham, and J.D. Rhoades. 1985a. Kinetics of post-reclamation boron dissolution. *Soil Sci. Soc. Am. J.* 49:836-839.
- Peryea, F.J., F.T. Bingham, and J.D. Rhoades. 1985b. Mechanisms for boron regeneration. *Soil Sci. Soc. Am. J.* 49:840-843.
- Pizer, R., and L. Babcock. 1977. Mechanism of the complexation of boron acids with catechol and substituted catechols. *Inorg. Chem.* 16:1677-1681.
- Rhoades, J.D., R.D. Ingvalson, and J.T. Hatcher. 1970. Adsorption of boron by ferromagnesian minerals and magnesium hydroxide. *Soil Sci. Soc. Am. Proc.* 34:938-941.
- Sharma, H.C., N.S. Pasricha, and M.S. Bajwa. 1989. Comparison of mathematical models to describe boron desorption from salt-affected soils. *Soil Sci.* 147:79-84.
- Sims, J.R., and F.T. Bingham. 1968a. Retention of boron by layer silicates, sesquioxides, and soil materials: II. Sesquioxides. *Soil Sci. Soc. Am. Proc.* 32:364-369.
- Sims, J.R., and F.T. Bingham. 1968b. Retention of boron by layer silicates, sesquioxides, and soil materials: III. Iron- and aluminum-coated layer silicates and soil materials. *Soil Sci. Soc. Am. Proc.* 32:369-373.
- Singh, S.P.N., and S.V. Mattigod. 1992. Modeling boron adsorption on kaolinite. *Clays Clay Miner.* 40:192-205.
- Sparks, D.L. 1989. Kinetics of soil chemical processes. Academic Press, San Diego.
- Sparks, D.L., and P.C. Zhang. 1991. Relaxation methods for studying kinetics of soil chemical phenomena. p. 61-94. *In* D.L. Sparks and D.L. Suarez (ed.) Rates of soil chemical processes. SSSA Spec. Publ. 27. SSSA, Madison, WI.
- Stumm, W., C.P. Huang, and S.R. Jenkins. 1970. Specific chemical interaction affecting the stability of dispersed systems. *Croat. Chem. Acta* 42:223-245.
- Stumm, W., R. Kummert, and L. Sigg. 1980. A ligand exchange model for the adsorption of inorganic and organic ligands at hydrous oxide interfaces. *Croat. Chem. Acta* 53:291-312.
- Westall, J., and H. Hohl. 1980. A comparison of electrostatic models for the oxide/solution interface. *Adv. Colloid Interface Sci.* 12:265-294.
- Westall, J.C. 1982. FITEQL. A program for the determination of chemical equilibrium constants from experimental data. Version 2.0. Dep. of Chemistry, Oregon State Univ., Corvallis.
- Yasunaga, T., and T. Ikeda. 1986. Adsorption-desorption kinetics at the metal-oxide-solution interface studied by relaxation methods. p. 230-253. *In* J.A. Davis and K.F. Hayes (ed.) Geochemical processes at mineral surfaces. Proc. ACS Annu. Meet. Geochemistry 190th, Chicago. 8-13 Sept. 1985. Am. Chem. Soc., Washington, DC.